Journal of Physics: Conference Series **353** (2012) 012008 doi:10.1088/1742-6596/353/1/012008

Approximations for acoustically excited bubble cluster dynamics

D Sinden, E Stride and N Saffari

Department of Mechanical Engineering, Roberts Building, Torrington Place, London, WC1E 7JE, United Kingdom

E-mail: d.sinden@ucl.ac.uk

Abstract. In this paper the effect of interaction on the expansion of a bubble in a regular monodisperse cluster is investigated. By a geometric construction a two-dimensional ordinary differential equation with an exact expression for first-order bubble interactions is derived for an n-bubble model. An approximate equation is derived for the rapid expansion of the bubble which can be solved yielding an analytic expression for the collapse of a bubble which undergoes inertial cavitation. It is then demonstrated that the maximum volume of a bubble in a cluster is considerably less than that of a single bubble. This result is of significance as typically the dispersion relationship, the wave speed and the co-efficient of attenuation are calculated using a single bubble model and summed for the total number of bubbles to yield the void fraction. Furthermore it is shown that the maximum radius of a bubble in the cluster is considerably smaller than that of a single bubble, yet the duration of the collapse phase is only weakly dependent on the number of bubbles. Hence, it is conjectured that the likelihood of fragmentation due to Rayleigh–Taylor instability is reduced. The results from the analysis are in good agreement with full numerical simulations of multi-bubble dynamics, as well as experimental observations

1. Introduction

It has long been known that when bubbles interact with each other, their dynamics are often significantly different from those of isolated bubbles, for example bubbles may attract or repel one another [1] or their collapse phases may synchronize [2]. There is a wide range of studies, both experimental [3, 4] and theoretical devoted to multi-bubble dynamics, by direct numerical simulations of few-bubble systems [5–9] or averaged cloud models [10–12].

There have been several studies, in which bubbly flows at nondilute, finite void fraction were investigated through effective equations intended to capture wave phenomena. There are essentially two approaches to the problem. The first approach was pioneered by Foldy [13], who derived a dispersion relation by treating wave propagation

in a bubbly mixture as a problem of multiple scattering by randomly distributed isotropic scatterers representing the spherical bubbles.

Alternatively, van Wijngaarden [14] introduced volume-averaged quantities which matched the microscopic conservation laws for each phase in order to remove the local fluctuations due to scattering and then derived the averaged equations based on heuristic, physical reasoning. Caflisch *et al.* [15, 16] rigorously extended the work of van Wijngaarden and proved that the relative motion between the bubbles and the liquid does not play a significant role, justifying the assumptions. Linear equations in the limits of weak applied forcing and small void fraction recovered the results of Foldy, by essentially replacing the complex distribution of gas bubbles and liquid with a continuous effective medium. From these linear equations Commander and Prosperetti [17] derived a dispersion relation.

Typically the dispersion relation and the co-efficient of attenuation are calculated using a single bubble model and summed for the total number of bubbles. As Leighton *et al.* [18] highlight, attenuation and wave speed are often measured in order to infer bubble size distributions. However, the derivation of the attenuation and wave speed are based on linear theory [17]. Thus accuracy in the measurement of the bubble size distribution is implicitly limited by the underlying assumptions that the bubbles must not collapse inertially, which is dependent on the bubble sizes. Ida [7] computed radius-time curves in coupled polydisperse bubble systems and observed that the maximum radius of smaller bubbles was reduced. This was attributed to the expansion of a bubble being suppressed by the pressure waves which larger neighbouring bubbles emit during their expansion.

The first estimations of the maximum radius of a single bubble were derived by Apfel and Holland [19, 20]. In a heuristic manner, the authors assumed that initially the bubble growth was linear, then dealt with the subsequent growth by equating the potential and kinetic energy of the bubble. Löfstedt *et al.* [21] and Hilgenfeldt *et al.* [22] demarcate the radius-time profile of a single bubble into distinct regions of expansion, collapse and afterbounce. Within each regime the dominant effects on the bubble were identified and reduced governing equations in each regime derived. In this paper, using geometric arguments [23] to reduce a $2n$-dimensional system of coupled interacting Rayleigh–Plesset type equations to an exact two-dimensional modified Rayleigh–Plesset equation, it will be demonstrated that for inertially collapsing bubbles the time-averaged volume of an n-bubble cluster will be significantly less than that of n isolated bubbles. Hence a more accurate approximation of a time-averaged void fraction may be derived. This is significant as experiments have shown that for water-air mixtures void fractions as low as 0.5% can lead to a drop in sound speed from 1500m/s to 160m/s, which is actually lower than the sound speed in air [24]. The explanation is that the sound speed depends on both the compressibility and the density of the medium. As the former is determined by the density of gas bubbles and the latter by the properties of the liquid, the resulting sound speed can vary drastically from that of either the liquid or the gas [25].

With the assumption of local homogeneity, Rubinstein [26] extended the approach derived in [15, 16] to a nonlinear analysis of periodic lattice multi-bubble system by homogenisation and derived an modified Rayleigh–Plesset equation, which includes

the effects of interactions. Beylich and Gülhan [27] used a correction factor for the bubble-bubble interaction effect by fitting the result of a model equation to experimental data for a bubbly shock flow. Kubota *et al.* [28] modelled the bubble-bubble interaction around a hydrofoil by adding the velocity potential of other bubbles. As Seo *et al.* [29] state most of the proposed models for the bubble-bubble interaction have not been critically validated and the proposed correction factors for bubble-bubble interaction vary dramatically, not only in magnitude but also in sign, from study to study. In [29] the authors also used a locally averaged volume averaged Rayleigh–Plesset equation and compared the results against direct numerical simulations using a front tracking method. The effects of interaction became noticeable at void fractions 1% and became significant beyond 10%. Reasonable agreement between averaged equations and direct numerical simulation was found for void fractions up to 13%. Yasui *et al.* [30] investigated inertial collapse within a bubble cloud and found that shock waves do not lead to broadband noise if the bubbles are shape-stable, but broadband noise can be attributed to temporal fluctuations in the number of bubbles within a cloud.

The outline of this paper is as follows, in section 2 the Rayleigh–Plesset equation is introduced and in subsection 2.1 the reduced set of governing equations based on geometrically exact constructions is presented. In section 3 an analytical expression which approximates the expansion phase of a bubble in cluster is derived. Finally, in section 4 the results are summarised and the implications discussed.

2. The Rayleigh–Plesset Equation

The Rayleigh–Plesset equation is an nonlinear ordinary differential equation which models the oscillations of a single gas filled spherical bubble of radius $R = R(t)$ whose centre is stationary. The Rayleigh–Plesset equation can be derived by balancing the energy supplied to the bubble by the incident pressure and the surrounding fluid to the kinetic energy of the bubble oscillations [21].

The interaction between two bubbles, R_i and R_j, a distance D_{ij} apart from their centres, due the re-radiated pressure field is given by Mettin *et al.* [31]. It is derived by matching the velocity field for an incompressible liquid with the pressure field using the conservation of momentum. On computing the interaction to first-order, neglecting terms of $\mathcal{O}\left(1/D^5\right)$ and $\mathcal{O}\left(1/cD\right)$, for n-bubbles the governing equation is given by the $2n$-dimensional equation

$$\rho\left(R_i\ddot{R}_i + \frac{3}{2}\dot{R}_i^2 + \sum_{\substack{j=1,\\ j\neq i}}^{n}\frac{R_j}{D_{ij}}\left(R_j\ddot{R}_j + 2\dot{R}_j^2\right)\right) = p_g\left(R_i\right) + p_v - p_\infty - \frac{2\sigma}{R_i} - \frac{4\mu\dot{R}_i}{R_i} + p\left(t\right). \tag{1}$$

Here ρ is the density of the surrounding (irrotational, infinite, incompressible) liquid, p_g is the internal pressure of the gas in the bubble given by

$$p_g\left(R\right) = \left(p_\infty - p_v + \frac{2\sigma}{R_0}\right)\left(\frac{R_0^3 - a^3}{R^3\left(t\right) - a^3}\right)^\kappa, \tag{2}$$

with p_∞ is the hydrostatic pressure, p_v is the vapour pressure, $R_0 = R(0)$ is the initial bubble radius, σ is the surface tension, κ is the polytropic exponent of the gas within the bubble, a is the hard-core van der Waals radius and μ is the shear viscosity of the liquid. The gas is assumed to be ideal, thus the internal pressure is a function of the bubble radius only, hence p_v is constant. The applied acoustic pressure takes the form

$$p(t) = p_a \sin(\omega t + \varphi_0) \tag{3}$$

where p_a is the magnitude of the pressure, ω is the driving frequency and φ_0 is the phase of the applied field. The internal conditions, such as vapour content and polytropic index and external conditions, such as the fluid density, viscosity, surface tension and ambient pressure are all assumed to be identical for each bubble.

In the derivation of the Rayleigh–Plesset equation it is assumed that the wavelength of the sound field is large in comparison with the radius of the bubble and that the motion of the bubble wall is slow in comparison with the speed of sound in the liquid and the gas. Diffusive, thermal and chemical effects are all neglected. Discussions of the underlying assumptions and limitations of the classical Rayleigh–Plesset equation are given in [21, 22].

In the case of interacting bubbles some further assumptions are necessary. Firstly, the fluid is assumed to be incompressible so that the interactions between bubbles are instantaneous. Secondly, the distances between bubbles are assumed to be sufficiently large so that the bubbles remain spherical [32]. For violently collapsing bubbles a shock-like pressure wave may be released [33] containing small-amplitude high-frequency components whose wavelengths may be of a comparable size to the bubbles. As the focus of this paper is on the behaviour of interacting bubbles during expansion this situation will not arise and so the assumptions underpinning the Rayleigh–Plesset equation are still valid.

2.1. Geometric Averaging

Although it is possible to generalise the Rayleigh–Plesset equation (1) to an n-bubble model, it is not possible to express the natural frequencies of the system analytically for an arbitrary n-bubble model if $n \geq 5$. However, if the system of n-interacting equally sized bubbles forms a complete graph, i.e. are arranged in a regular polygon planar to the incident wave, the Rayleigh–Plesset equation can be simplified by exploiting the invariance of the dihedral symmetry group. The physical interpretation is that although the distances between pairs of bubbles are different, and thus the magnitude of the pressure waves due to interactions different, the sum of the distances between a bubble and all of its neighbours will be the same for every bubble, as is illustrated in Fig. 1. Thus the total incident pressure wave due to interaction will be the same for every bubble. Hence the Rayleigh–Plesset equation can be generalised to incorporate the multiple bubble interactions via

$$R_j \mapsto R \quad \text{and} \quad \sum_{\substack{j=1,\\ j\neq i}}^{n} \frac{R_j}{D_{ij}} \left(R_j \ddot{R}_j + 2\dot{R}_j \right) \mapsto \frac{\alpha_n}{D} R \left(R\ddot{R} + 2\dot{R}^2 \right) \tag{4}$$

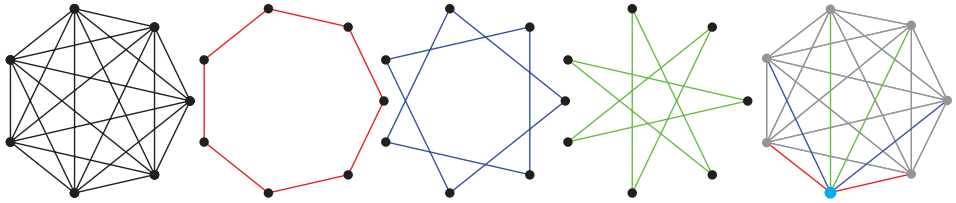

Figure 1: The interactions of a set of equally sized bubbles arranged in a heptagon ($n = 7$) form a complete graph which can be decomposed into three star polygons which connect with the first, second and third nearest neighbour. Each star polygon has a unique length scale λ_i, $i = 1, 2, 3$. The total interaction force on a bubble is given a sum of the length scales weighted by the total number of interactions per length scale.

where α_n is a dimensionless weighting parameter for the interaction amongst the n-bubbles and D is the distance between a bubble and its nearest neighbour. The dimension of the governing equation is thus independent of the number of bubbles and can be reduced from a $2n$-dimensional system to a two-dimensional system. Hence, for a single bubble $\alpha_1 = 0$ as there is no interaction, for a pair of bubbles $\alpha_2 = 1$, for three bubbles arranged in an equilateral triangle $\alpha_3 = 2$, for a square array of bubbles

$$\frac{1}{D} + \frac{1}{D} + \frac{1}{\sqrt{2}D} = \frac{1}{D}\left(2 + \frac{1}{\sqrt{2}}\right) \Rightarrow \alpha_4 = \frac{1 + 2\sqrt{2}}{\sqrt{2}} \tag{5}$$

and for a regular pentagon the sum of the internal lengths gives

$$\frac{1}{D} + \frac{1}{D} + \frac{1}{D\left(1 + \sqrt{5}\right)/2} + \frac{1}{D\left(1 + \sqrt{5}\right)/2} \Rightarrow \alpha_5 = \frac{2\left(3 + \sqrt{5}\right)}{1 + \sqrt{5}} \tag{6}$$

and so on. Fig. 1 illustrates the length scales of the heptagon, which is the first regular polygon whose length scales can not all be expressed by real numbers.

Rather than by repeatedly applying trigonometric formulae for each regular array, the procedure can be generalised by noting that the sum of all the interactions forms a complete graph which can be decomposed into star polygons. The i^{th}-star polygon has an associated length scale, λ_i, based only on the total number of bubbles and the minimum distance between any two bubbles. Each of the length-scales may be found via the roots of Chebyshev polynomials [23]. The total interaction force on a bubble is given by the sum of the length scales, λ_i, weighted by the total number of interactions per length scale, which is denoted by ϕ_i. The parameter α_n can expressed as

$$\alpha_n = \sum_{i=1}^{n} \frac{D}{D_i} - 1 = \sum_{i=1}^{n} \phi_i \lambda_i - 1 \tag{7}$$

where the subtraction is due to the fact that when $n = 1$ there will be no interaction. When $n = 2k + 1$ the length scales λ_i are the n positive roots of the polynomial $u_n = u_n\left(1 - \lambda^2/2\right)$ where $u_n(\cdot)$ is an n^{th}-order Chebyshev polynomial of the

second kind. When $n = 2k$ then λ_i are found as the positive roots of $v_n = v_n\left(1 - \lambda^2/2\right)$ where $v_n = u_n + u_{n-1}$. For the case of $n = 2k + 1$ equally sized bubbles there will be $2k$ interactions so each length scale will be equally weighted as there will be two interactions every length scale. However for $n = 2k$ equally sized bubbles there will be $2k - 1$ interactions, where, on the largest length scale, the bubble interacts with a single bubble. The parameter ϕ_i is given by the following relation

$$\text{if} \quad n = \begin{cases} 2k & \text{then} \quad \phi_i = 2 \\ 2k+1 & \text{then} \quad \phi_i = \begin{cases} 2 & \text{for} \quad i = 1, \ldots, 2k \\ 1 & \text{for} \quad i = 2k+1. \end{cases} \end{cases}$$

Hence, for regular configurations, the dimension of the system is reduced to a two-dimensional modified Rayleigh–Plesset equation of the form

$$\rho\left(R\ddot{R} + \frac{3}{2}\dot{R}^2 + \frac{\alpha_n R}{D}\left(R\ddot{R} + 2\dot{R}^2\right)\right) = p_g\left(R\right) + p_v - p_\infty - \frac{2\sigma}{R} - \frac{4\mu\dot{R}}{R} + p\left(t\right) \tag{8}$$

which, on linearisation, yields a single natural frequency, given by

$$\omega_0 = \sqrt{\frac{1}{\rho\left(1 + R_0\alpha_n/D\right)}\left(\frac{3\kappa\left(p_\infty - p_v\right)R_0}{R_0^3 - a^3} + 2\sigma\left(\frac{3\kappa}{R_0^3 - a^3} - \frac{1}{R_0^3}\right)\right)}. \tag{9}$$

An increase in the number of bubbles increases α_n and, therefore, reduces the natural frequency of the system, in agreement with experimental observations [34]. However, in the limit $n \to \infty$ the formulation is of limited applicability as the configuration approaches a circle of infinite radius.

The averaging of the bubble interactions has previously been attempted by Yasui *et al.* [4, 30] and Kubota *et al.* [28], who assumed the bubble cloud to be monodisperse and made a "crude" approximation based on the averaging of the geometric configuration of the bubble cloud for the coupling strength S

$$R_j \mapsto R \quad \text{and} \quad \sum_{\substack{j=1, \\ j\neq i}}^{n} \frac{R_j}{D_{ij}}\left(R_j\ddot{R}_j + 2\dot{R}_j\right) \mapsto SR\left(R\ddot{R} + 2\dot{R}^2\right),$$

where the coupling strength is approximated as

$$S = S_i = \sum_{j=1}^{n-1} \frac{1}{D_{ij}} \approx 4n\pi \int_{l_{\min}}^{l_{\max}} r \, \mathrm{d}r \approx 2n\pi l_{\max}^2 \tag{10}$$

with $l_{\min} \ll l_{\max}$ the distances to the nearest and furthest bubbles for a bubble in the cluster. Yasui *et al.* estimated that the coupling strength could be of the magnitude 10^6/m in the homogeneous bubble cloud found in ultrasonic cavitation at large pressures, 2.9atm.

While the assumption of geometric regularity is somewhat unphysical, the primary benefit of the assumptions is the reduction in the dimension of $2n$-dimensional system

to a two-dimensional system, allowing many analytical techniques from single bubble theory to be carried over. However, numerical simulations on the two-dimensional Rayleigh–Plesset equation (8) suggest that the geometric formulation is robust under perturbation in that if the bubbles are arranged in a regular array and the location of each bubble is perturbed slightly in the plane of the wave, each radius-time profile will be perturbed form the radius-time profile of the bubbles regular array by a small amount. However, whether the spatial perturbation is robust for consequent translational motion under the primary Bjerknes force is not yet known.

If compressibility was incorporated in the Rayleigh–Plesset equation then delays would be included in the bubble-bubble interaction but the system would still be two-dimensional, where the delays would be given by $\tau_i = D_i/c = \alpha_i D/c$.

Although the likelihood of nucleation occuring in a regular array in an uncontrolled environment is highly unlikely, nucleation in a regular array can be performed in a controlled and repetable manner. Kroon *et al.* [35] induced cavitation using an array of laser foci by shaping a pulsed laser beam using a digital hologram and focusing it into a small volume of liquid. Bremond *et al.* [36] used a hydrophobic surface patterned with micro-cavities as nucleation sites when the liquid pressure is lowered. In both cases the authors showed that the dynamics of the clusters were in good agreement with analytical models if the bubbles remained spherical. However, if the separation distance was beyond the threshold derived by Zavtrak [32], the interaction would lead to non-spherical collapse and jetting towards the centre of the arrays.

Figure 2 illustrates a radius-time profile for a one, two and three bubble clusters, where density is given by $\rho = 1000\text{kg/m}^3$, hydrostatic pressure $p_\infty - p_v = 1\text{atm}$, surface tension $\sigma = 0.073\text{kg/m}^2$, polytropic index $\kappa = 5/3$, van der Waals radius $a = 8.85$, frequency $\omega = 2\pi \cdot 27\text{kHz}$ and applied pressure $p_a = 1.36\text{atm}$. The figure clearly shows that the maximum radius decreases as the number of bubbles increases for a bubble in the cluster.

3. Approximating the Expansion Phase

By geometric arguments, the dimension of the multi-bubble system is reduced from a $2n$-dimensional system to a two-dimensional system and is thus far more amenable to analysis. In this section an analytical estimate for the expansion phase of the bubble is derived. As Fig. 2 illustrates, the expansion phase of a bubble will account for a significant part of the time-averaged volume of a bubble. Thus an estimation of the bubble radius during this phase has utility in predicting the attenuation for example.

During the expansion phase, the governing equation is dominated by the inertial terms and the driving pressure. The expansion phase of a bubble is determined by the time in which the applied acoustic pressure is negative. From Fig. 3 let

$$t_- = \frac{1}{\omega}\sin^{-1}\left(\frac{p_\infty - p_v}{p_a}\right) \quad \text{and} \quad t_+ + t_- = \frac{\pi}{\omega} \tag{11}$$

so that (t_-, t_+) is the interval in which the total acoustic pressure on the bubble is negative. Note that an inertially collapsing bubble may continue to expand when the applied pressure field is positive due to its own momentum, before collapsing at time $t_{\min}$ [37]. Thus, the inertial terms in the Rayleigh–Plesset equation, and the applied

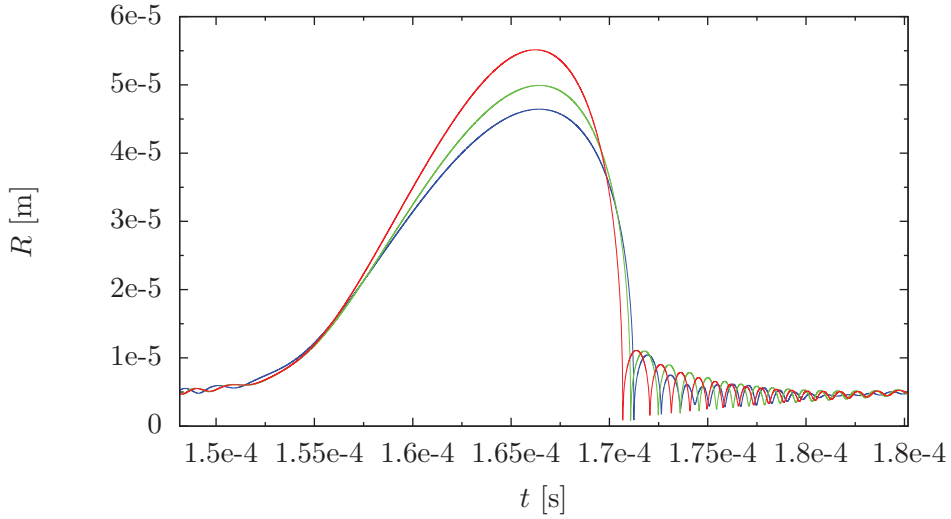

Figure 2: Radius-time profiles for a single bubble (red), two (green) and three (blue) bubbles of initial radius $R_0 = 5\mu$m with $\rho = 1000\text{kg/m}^3$, $p_\infty - p_v = 1\text{atm}$, $\sigma = 0.073\text{kg/m}^2$, $\kappa = 5/3$, $a = 8.85$ under acoustic field with $\omega = 2\pi \cdot 27\text{kHz}$ and $p_a = 1.36\text{atm}$. Note that the maximum amplitude decreases as the number of bubbles increases. The radius-time profiles displayed are from the fifth acoustic cycle, so that transient oscillations have passed.

acoustic pressure are the significant terms during the expansion and beginning of the collapse phase.

The inertial terms may be written as

$$R\ddot{R} + \frac{3}{2}\dot{R}^2 = \frac{3}{4}\frac{\mathrm{d}^2}{\mathrm{d}t^2}R^2 - \frac{1}{2}R\ddot{R} \tag{12a}$$

or as

$$R\ddot{R} + \frac{3}{2}\dot{R}^2 = \frac{1}{2}\frac{\mathrm{d}^2}{\mathrm{d}t^2}R^2 + \frac{1}{2}\dot{R}^2. \tag{12b}$$

Numerical simulations [22] show that, as observed in [19], in the interval $t \in (t_-, t_+)$ the velocity of the bubble is the dominant effect as the growth is almost linear. Whereas in the interval $t \in (t_+, t_{\min}]$, that is when the bubble reaches it maximum radius and collapses, it is the acceleration of the bubble which is the dominant effect. Thus in the two domains, the weaker contributions to the expansion can be neglected.

The complete effect of interaction can be included in both regimes by exploiting the fact that the interaction is an exact second derivative, i.e.

$$\frac{\alpha_n}{D}R\left(R\ddot{R} + 2R\dot{R}^2\right) = \frac{\alpha_n}{3D}\frac{\mathrm{d}^2}{\mathrm{d}t^2}R^3. \tag{13}$$

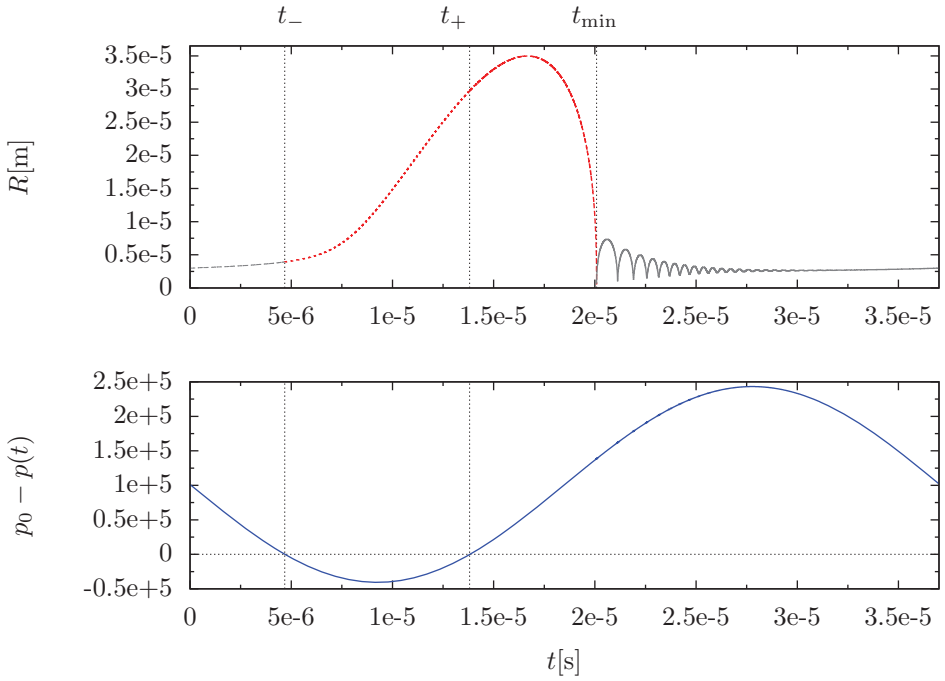

Figure 3: Regimes in which expansion phase of bubble is modelled, showing the effective applied acoustic wave and the times which determine the bubble expansion (11). In this figure $R_0 = 3\mu$m and $p_a = 1.36$atm. In the radius-time profile, the numerical solution on the domains (t_-, t_+) and $(t_-, t_{\min}]$ are shown by the red dotted and red dashed lines respectively.

Hence, following [22] and [38], the expansion phase can be formulated as

$$\frac{3\rho}{4}\frac{\mathrm{d}^2}{\mathrm{d}t^2}\left(R^2\left(1+\frac{4\alpha_n}{9D}R\right)\right) = p_a\sin(\omega t) - A + \mathcal{O}\left(R\ddot{R}\right) \quad \text{on} \quad (t_-, t_+) \quad \text{as} \quad \dot{R}^2 \gg R\ddot{R} \tag{14a}$$

and

$$\frac{\rho}{2}\frac{\mathrm{d}^2}{\mathrm{d}t^2}\left(R^2\left(1+\frac{2\alpha_n}{3D}R\right)\right) = p_a\sin(\omega t) - A + \mathcal{O}\left(\dot{R}^2\right) \quad \text{on} \quad (t_+, t_{\min}] \quad \text{as} \quad \dot{R}^2 \ll R\ddot{R} \tag{14b}$$

where A is given by

$$A = p_0 - \frac{2\sigma}{R_0}\frac{1}{K(p_0, p_a)} \quad \text{with} \quad p_0 = p_\infty - p_v \tag{15}$$

and K is a constant effective surface tension, dependent only on the ambient and applied pressures. The effective surface tension shall be determined later.

Denoting the solution over the range (t_-, t_+) as $R_-(t) = R(t)$, the first equation can be solved on the domain by integrating twice, with the initial conditions $R_-(t_-) = \zeta R_0$

and $\dot{R}_-(t_-) = \omega\zeta R_0$, where $\zeta = 1.6$ is a matching parameter inferred from full numerical simulations. Thus on (t_-, t_+) the governing equation is given by

$$R_-^2\left(1+\frac{4\alpha_n}{9D}R_-\right) = \frac{4}{3\rho\omega^2}\left(p_0 - p_a\sin\omega t + p_a\omega\left(t-t_-\right)\cos\omega t_- - \frac{A}{2}\omega^2\left(t-t_-\right)^2\right) + \zeta^2 R_0^2\left(1+\frac{4\alpha_n}{9D}\zeta R_0 + 2\omega\left(1+\frac{2\alpha_n}{3D}\zeta R_0\right)\left(t-t_-\right)\right). \tag{16a}$$

Solving the equation on the next domain $(t_+, t_{\min}]$ for $R_+(t) = R(t)$, by enforcing that R is derivative is continuous at t_+, i.e. $R_-(t_+) = R_+(t_+)$ and $\dot{R}_-(t_+) = \dot{R}_+(t_+)$, yields

$$R_+^2\left(1+\frac{2\alpha_n}{3D}R_+\right) = \frac{2}{\rho\omega^2}\left(p_0 - p_a\sin\omega t + p_a\omega\left(t-t_+\right)\cos\omega t_+ - \frac{A}{2}\omega^2\left(t-t_+\right)^2\right) + c_1\left(t-t_+\right) + c_2 \tag{16b}$$

where the constants

$$c_1 = 2\dot{R}_-(t_+)R_-(t_+)\left(1+\frac{\alpha_n}{D}R_-(t_+)\right) \quad \text{and} \quad c_2 = R_-^2(t_+)\left(1+\frac{2\alpha_n}{3D}R_-(t_+)\right) \tag{17}$$

ensure continuity. Closed form expressions for the radius during expansion can be found by solving a cubic equation, but are overly complicated and are omitted for brevity. However, for a single bubble the solution can be written as

$$R_+^2(t) = \frac{2}{\rho\omega^2}\left(p_0 - p_a\sin\omega t + p_a\omega\left(\frac{1}{3}t+t_+\right)\cos\omega t_+ - \frac{A}{2}\omega^2\left(t^2+t_+^2+\frac{2}{3}tt_+\right)\right) + \zeta^2 R_0^2\left(1+2\omega\left(t+t_+\right)\right) \tag{18}$$

It is important to note that at the instance of collapse the model breaks down, with all solutions unphysical. That is, the roots of the cubic are a pair of complex conjugates and negative real root. The instance of collapse can be crudely approximated by setting the right-hand side of Eq. (16b) equal to zero and solving for $t_{\min}$. Although this provides a reasonably accurate approximation for the collapse time, during the latter part of the collapse phase the model neglects effects such as internal pressure which become comparable to the inertial terms when arresting the collapse of the bubble.

The maximum radius $R_{\max} = R_+(t_{\max})$ can be found by setting $\dot{R}_+(t) = 0$ to yield an implicit expression for the time $t = t_{\max}$, which can be substituted into Eq. (16b). The time at which the radius of the bubble is maximal is found via numerical solutions to the transcendental equation

$$\frac{1}{\rho\omega^2}\left(p_a\cos\omega t_{\max} + p_a\cos\omega t_+ - A\omega\left(t_{\max}-t_+\right)\right) + c_1 = 0. \tag{19}$$

There is only one root to equation (19) in the domain $(t_+, t_{\min}]$, as in the limit $t \to t_{\min}$ the radius tends to zero, $R_+(t) = 0$.

The transition radius R_{trans} is the initial radius which demarcates weakly oscillating bubbles from bubbles which undergo rapid expansion. Hilgenfeldt [22, Fig. 7] showed numerically that for an inertially collapsing bubble, that is when $p_a \gg p_0$, the ratio of the maximum radius to the initial radius was constant when the initial radius was close to the transition radius. Thus

$$\frac{\partial}{\partial R_0}\left(\frac{R_{\max}(p, R_0)}{R_0}\right)\bigg|_{R_0=R_{\text{trans}}} = 0 \quad \text{with} \quad R_{\text{trans}} = \frac{4\sigma}{3(p_0 - p_a)}. \tag{20}$$

Following Hilgenfeldt's analysis it is simple to show that the transition radius is independent of the number of bubbles. Hence, the effective surface tension can now be approximated by matching the transition radius with the maximum of the nondimensional function $R_{\max}/R_0$.

The maximum radius was found by solving Eq. (19), without dependence on ζ or the effective surface tension K, that is $A = p_0$. Trigonometric terms can be expanded to first-order to give

$$t^{(0)}_{\max} = \frac{1}{\omega p_0}\left(p_a + \frac{1}{3}\left(p_a \cos\omega t_+ - p_0 \omega t_+\right)\right) \tag{21}$$

which depends only on the applied and ambient pressures. In [38] the procedure was extended to higher-orders. Again, neglecting the effects of surface tension, equation (19) is solved and trigonometric terms expanded to second-order as

$$t^{(1)}_{\max} = \frac{1}{\omega}\left(\frac{p_a}{p_0} + \sqrt{\frac{2}{p_a}\left(\omega p_0 t^{(0)}_{\max} + 3\omega^2 \rho c_1 + \frac{p_0^2}{2p_a}\right)}\right) \tag{22}$$

which now depends on R_0 and through c_1 on α_n, as well as the applied and ambient pressures. However, it is assumed that the dependence on R_0 is weak, so that $\partial t^{(1)}_{\max}/\partial R_0$ can be neglected. Thus expression (22) can be substituted in Eq. (16b) to give the maximum radius and the condition (20) applied to yield an expression for the effective surface tension. When $\alpha_n = 0$ the effective surface tension can be written in the simple form

$$K(p) = \frac{3t^2_{\max} + 3t_+ + 2t_{\max}t_+}{g(p, t_{\max})}\frac{3}{4\sqrt{3}}(p-1) \quad \text{with} \quad t_{\max} = t^{(1)}_{\max} \tag{23}$$

where

$$g(p,t) = \frac{2}{\rho\omega^2}\left(p_0 - p_a \sin\omega t + p_a\omega\left(\frac{1}{3}t + t_+\right)\cos\omega t_+\right). \tag{24}$$

However, when interaction is considered the expression for the effective surface tension becomes far more complicated.

From the analysis, the time when the radius of the bubble is largest is very weakly dependent on the number of bubbles, which is also illustrated by the full numerical simulations of the Rayleigh-Plesset equation (8) in Fig. 2. The maximum radius is strongly influenced by the number of bubbles. The maximum radius $R_{\max}$ is found by

substituting the value of the collapse time into the expression (16b) and solving the cubic equation for $R_{\max}$. Typically, there is a positive real root and a pair roots those real part is always negative. The positive real root of the cubic is a monotonically decreasing function with respect to α_n/D. Thus effect of interaction decreases the time-averaged size of the bubble.

Numerical calculations, illustrated in Fig. 4 clearly show that the approximations are in good agreement with the full numerical simulations up to the point of collapse.

The maximum radius for small multi-bubble clusters is shown in Fig. 5. The reduction in the maximum radius due to the influence of interaction is clear, in good agreement with those observed in [7]. Note that the calculations hold over a portion of a single acoustic cycle, so that if a bubble displays characteristics of chaotic behaviour, such as a period-doubling and sensitivity to initial conditions, then these will not be directly observed in the analysis. However, if a bubble is oscillating chaotically this can be incorporated into the analysis by letting ζ be a random variable for each acoustic cycle.

Towards the end of the inertial collapse phase while the acceleration is positive, that is while the gas is still accelerating into the fluid, any non-spherical perturbations will grow exponentially and shape instability may develop during this brief time. This mechanism of instability is known as the Rayleigh–Taylor instability [39]. As the times at which the bubble reaches its maximum and minimum amplitudes of oscillation are weakly influenced by the number of bubbles, yet the maximum amplitude decreases noticeably as the number of bubbles increases, the analysis suggests that the influence of the interaction may soften the collapse. Thus, due to the influence of the interactions the likelihood of Rayleigh–Taylor instability should be reduced.

4. Conclusion

In this paper the interaction of a cluster of equally sized bubbles is investigated. If the bubbles are arranged in a regular array, planar to the applied acoustic field, then for each bubble the sum of the re-radiated pressure fields are equal, thus the governing equation for a bubble cluster can be reduced from an arbitrarily large $2n$-dimensional system to a single second-order modified Rayleigh–Plesset differential equation. Furthermore, the first-order interactions of bubbles arranged in a regular array can be calculated exactly using Chebyshev polynomials of the second kind. As the number of bubbles increases, the natural frequency of the cloud decreases, in agreement with existing experimental observations. The expansion phase of the bubble in a multi-bubble model is approximated by exploiting the observation that the first-order interaction is an exact differential. From the approximate equation, the expansion phase for a bubble in the cluster is found explicitly. Thus a time-averaged void fraction can easily be derived. The maximum radius can be found by solving for the time at which the bubble radius is stationary. An expression for the time at which the bubble radius is maximal is derived and solved numerically. It is observed that the time of maximum expansion is weakly dependent on the number of bubbles, which is also seen from full numerical simulations of the Rayleigh–Plesset equation. On substituting the time of maximum expansion into the expression for the expansion, the maximum radius can be calculated. This expression is influenced by the number of bubbles, again in good agreement with full numerical simulations of the Rayleigh–Plesset equation. As the maximum amplitude of oscillation

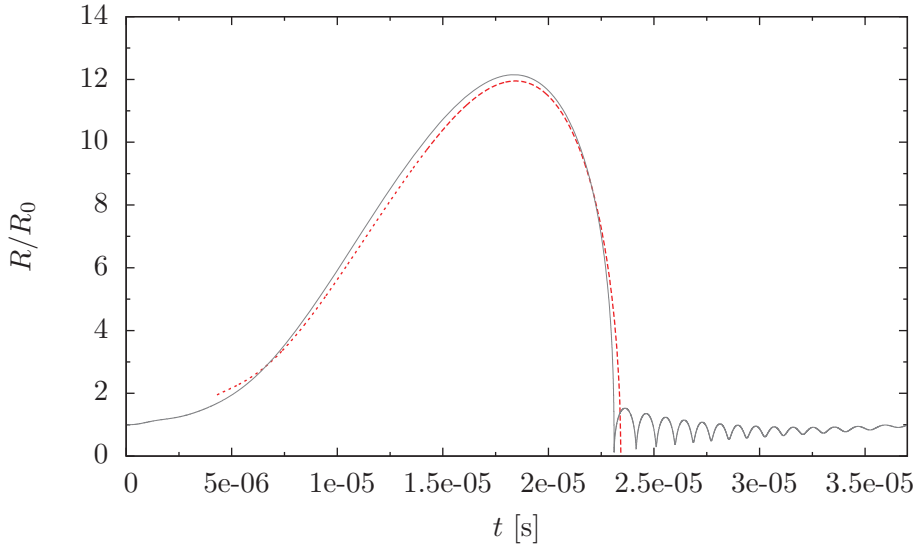

Figure 4: Comparison of analytical solution given by Eq. (16) and full numerical simulation (8) for a single bubble of size $R_0 = 5\mu$m with parameters given as in Fig. 2.

is reduced but the time between maximum to minimum radii essentially remains the same, it is conjectured that the likelihood of Rayleigh–Taylor instability developing may be reduced.

The analysis is complicated by the fact that the interaction is an exact differential yet approximations are made for the inertial terms of the bubble over two time domains. For a single bubble the expansion phase was modelled by a pair of differential equation whose inhomogeneous forcing terms had different co-efficients. Now, in the two domains, the third-order differentials also differ, cf. (16). An alternative would be to make the same assumptions for the interaction as are made for the inertial terms of the bubble, and thus approximate the interaction. However, this does not simplify the analysis as closed form expressions for the expansion are still given by the roots of a cubic equation, with a decrease in the accuracy of approximation.

Acknowledgments
This work was supported by the EPSRC under grant EP/F025750/1 and is gratefully acknowledged.

References

[1] Harkin A, Kaper T J and Nadim A 2001 *J. Fluid Mech.* **445** 377–411

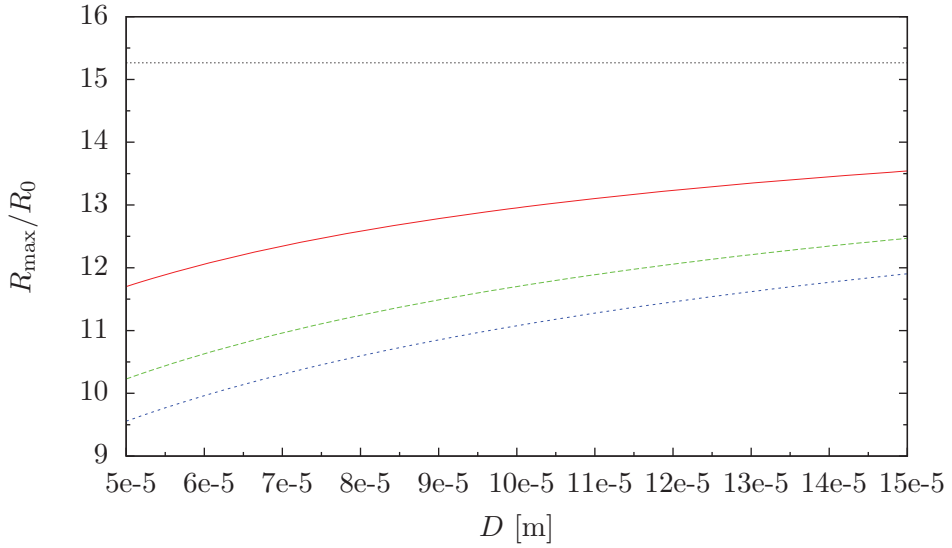

Figure 5: Ratio of maximum amplitude of the bubble radius and the initial radius for single (dotted), two (red solid), three (green/long-dash) and four (blue/short-dash) bubble clusters as the separation distance between the bubbles varies.

[2] Tervo J T, Mettin R and Lauterborn W 2006 *Acust. – Acta Acust.* **92** 178–180 ISSN 1610-1928

[3] Hatanaka S, Yasui K, Kozuka T, Tuziuti T and Mitome H 2002 *Ultrasonics* **40** 655–660

[4] Yasui K, Iida Y, Tuziuti T, Kozuka T and Towata A 2008 *Phys. Rev. E* **77** 16609

[5] Takahira H, Yamane S and Akamatsu T 1995 *JSME Int. J., Ser. B* **38** 432–439

[6] Ida M 2009 *Phys. Rev. E* **79** 16307

[7] Ida M 2009 *Phy. Fluids* **21** 113302

[8] Macdonald C A and Gomatam J 2006 *Proc. IMechE. C: J. Mech. Eng. Sci.* **220** 333–343

[9] Chong K J Y, Quek C Y, Dzaharudin F, Ooi A and Manasseh R 2010 *J. Sound Vib.* **329** 687–699

[10] Akhatov I, Parlitz U and Lauterborn W 1994 *J. Acoust. Soc. Am.* **96** 3627–3635

[11] Akhatov I, Parlitz U and Lauterborn W 1996 *Phys. Rev. E* **54** 4990–5003

[12] Parlitz U, Mettin R, Luther S, Akhatov I, Voss M and Lauterborn W 1999 *Phil. Trans. R. Soc. A* 313–334

[13] Foldy L L 1945 *Phys. Rev.* **67** 107–119

[14] van Wijngaarden L 1972 *Annu. Rev. Fluid Mech.* **4** 369–396
[15] Caflisch R E, Miksis M J, Papanicolaou G C and Ting L 1985 *J. Fluid Mech.* **153** 259–274
[16] Caflisch R E, Miksis M J, Papanicolaou G C and Ting L 1985 *J. Fluid Mech.* **160** 1–14
[17] Commander K W and Prosperetti A 1989 *J. Acoust. Soc. Am.* **85** 732–746
[18] Leighton T G, Meers S D and White P R 2004 *Proc. R. Soc. A* **460** 2521–2550
[19] Apfel R E 1986 *IEEE Trans. Ultrason., Ferroelect., Freq. Contr.* **33** 139–142
[20] Holland C K and Apfel R E 1989 *IEEE Trans. Ultrason., Ferroelect., Freq. Contr.* **36** 204–208
[21] Löfstedt R, Barber B P and Putterman S J 1993 *Phy. Fluids* **5** 2911–2928
[22] Hilgenfeldt S, Brenner M P, Grossmann S and Lohse D 1998 *J. Fluid Mech.* **365** 171–204
[23] Savio D Y and Suryanarayan E R 1993 *Am. Math. Monthly* **100** 657–661
[24] Smereka P 2002 *J. Fluid Mech.* **454** 287–325
[25] Sangani A S 1991 *J. Fluid Mech.* **232** 221–284
[26] Rubinstein J 1985 *J. Acoust. Soc. Am.* **77** 2061–2066
[27] Beylich A E and Gülhan A 1990 *Phy. Fluids* **2** 1412–1428
[28] Kubota A, Kato H and Yamaguchi H 1992 *J. Fluid Mech.* **240** 59–96
[29] Seo J H, Lele S K and Tryggvason G 2010 *Phy. Fluids* **22** 063302
[30] Yasui K, Tuziuti T, Lee J, Kozuka T, Towata A and Iida Y 2010 *Ultrason. Sonochem.* **17** 460–472
[31] Mettin R, Akhatov I, Parlitz U, Ohl C D and Lauterborn W 1997 *Phys. Rev. E* **56** 2924–2931
[32] Zavtrak S T 1987 *Akust. Zh.* **33** 240–242
[33] Matula T J, Hallaj I M, Cleveland R O, Crum L A, Moss W C and Roy R A 1998 *J. Acoust. Soc. Am.* **103** 1377–1382
[34] Kozhevnikova I N and Bjørnø L 1992 *Ultrasonics* **30** 21–25
[35] van der Kroon I, Quinto-Su P A, Li F and Ohl C D 2010 *Phys. Rev. E* **82** 066311
[36] Bremond N, Arora M, Ohl C D and Lohse D 2006 *Phys. Rev. Lett.* **96** 224501
[37] Flynn H G 1975 *J. Acoust. Soc. Am.* **57** 1379–1396
[38] Louisnard O 2008 *Phys. Rev. E* **78** 36322 ISSN 1550-2376
[39] Lin H, Storey B D and Szeri A J 2002 *Phy. Fluids* **14** 2925